Synthesis and Characterization of Aluminum-Rich Nanocomposite Powders at Cryogenic Temperatures

Carlo Badiola, Mirko Schoenitz, Xiaoying Zhu, Edward L. Dreizin
New Jersey Institute of Technology, Newark, NJ 07103

Abstract: Nanocomposite materials with reactive components are of interest for many applications in pyrotechnics, explosives, and propellants. Several such materials have been recently prepared by Arrested Reactive Milling (ARM), a method based on mechanical milling of μm-sized component powders to form μm-sized composite particles in which the components are mixed on a scale of 100 nm or finer. The temperature at which the milling is performed affects significantly both the rate at which the material is refined and the final properties of the product. In the present paper we report on an effort prepare Al-CuO and Al-MoO_3 reactive nanocomposites at cryogenic temperatures. A SPEX Certiprep 6815 Freezer/Mill was used to prepare the nanocomposites with aluminum-rich compositions from μm-sized component powders. The material was processed in steel vials using steel balls of different sizes as milling medium. The number and dimensions of the milling balls as well as the milling time were systematically varied. The prepared powders were characterized by X-ray diffraction, particle size analysis, and scanning electron microscopy. Thermal characteristics were studied using a custom wire-ignition setup and differential scanning calorimetry. Preliminary results show that the uniformity of mixing and reactivity of the nanocomposite powders can be substantially improved using milling at cryogenic temperatures.

I. Introduction

Nanocomposite reactive materials, in particular, thermites, are gaining much attention after recent studies showing that high reaction rates are possible to achieve in addition to the substantial reaction enthalpy when the reactive components are mixed on the scale of about 100 nm, see, for example refs. [1-7]. Among different techniques used to prepare such nanocomposite materials, Arrested Reactive Milling (ARM) method offers an inexpensive and scalable technique that is very versatile and can be applied to a wide range of reactive material compositions [8-13]. The ARM-prepared powders comprise micron-sized particles, where each particle is a fully dense composite with nano-sized inclusions of one component embedded in a matrix of the second component. The powders are prepared by high-energy mechanical milling of micron-sized powders of the individual components. Both a shaker mill and a planetary mill operated at room temperature were used in previous studies to prepare reactive nanocomposite materials by ARM. The milling is interrupted (or arrested) before the highly exothermic and typically self-sustaining reaction between the material components is triggered mechanically. Previous work showed that a slight reduction in the temperature at which the reactive materials are milled results in a substantial change in the product properties[14]. In parallel, substantial efforts have been reported on mechanical alloying performed at cryogenic temperatures[15,16]. The material properties, altered at cryogenic temperatures result in better-refined structures produced during shorter milling times. In some experiments, the phase make up of the mechanically alloyed compound was observed to be different depending on the milling temperature. Mechanical alloying, as ARM, relies on high-energy ball milling to refine the material structure. The key differences of ARM are that the starting components are capable of highly exothermic reaction and that the initiation of such a reaction or its precursors is undesirable. Thus, it is expected that ARM performed at cryogenic temperatures can result

in a very attractive combination of intimately refined reactive components for which the low processing temperature suppresses chemical interaction. This paper investigates the feasibility of preparation reactive nanocomposite materials by ARM at a cryogenic temperature.

II. Experimental

The experiments in this study were performed on a SPEX Certiprep 6815 Freezer/Mill. In this vibratory mill, four stainless steel vials are arranged horizontally, while submerged in liquid nitrogen. Two solenoids impose an alternating magnetic field that moves the magnetic milling media back and forth along the axis of the milling vials. Collisions occur among the milling media and between the media and the end caps of the milling vials. Available milling media were single cylindrical impactors, and hardened steel balls of varying diameter.

Initially, a $12Al{\cdot}MoO_3$ nanocomposite powder that had been previously prepared in a planetary mill was cryogenically milled to alter its particle size distribution. Later, aluminum (-325 mesh, <45 μm, 99.5%, Atlantic Equipment Engineering), and CuO (25 μm, 99+%, Sigma Aldrich), or MoO_3 (98%, Alfa Aesar) were placed in the milling vials directly to prepare nanocomposite powders with overall compositions of $12Al{\cdot}3CuO$, and $12Al{\cdot}MoO_3$, respectively. These metal-rich thermite compositions, which are substantially less reactive than stoichiometric compositions, were selected for initial cryogenic milling experiments in order to minimize possible damage to the equipment in case of undesirable thermite reaction occurring during the milling. Milling vials were loaded at room temperature in ambient air. The milling vials consist of stainless steel tubes which are closed off at the ends by loosely-fitting end caps. The end caps do not seal hermetically; therefore loading in a protective atmosphere was not attempted. After loading, the vials were pre-cooled by immersing in liquid nitrogen.

Milling parameters varied in experiments were the milling time, the frequency of the magnetic field, the type, mass, and number of the milling media, and the amount of powder in each vial. Details of the experiments are shown in Table 1.

Table 1: Overview of milling parameters

Composition	Powder Load, g	Milling Media	Milling Time, min	Frequency, Hz
$12Al{\cdot}MoO_3$, prepared in planetary mill	1.5 3	Cylindrical steel impactor 3/8" diameter by 2 3/8" length Steel balls: 3×1/2"; 7×3/8"; 58×3/16"	10 20 300	10 15
$12Al{\cdot}3CuO$, $12Al{\cdot}MoO_3$, direct milling	3	Steel balls: 3·7/16"; 58·3/16"; 3·7/16" + 10·3/16"	30 - 1200	15

The lack of a tight seal on the milling vials posed a significant problem, as during milling as much as 2/3 of the powder load was lost in some experiments. Likewise, unknown amounts of liquid nitrogen would enter the vials, changing the milling environment in poorly controllable ways. To alleviate this problem, the end caps were dipped in water before inserting into the ends of the vials. The water then filled the small gap between end cap and vial, and on freezing provided an effective seal. Material loss was reduced down to 0.3 % over a 20-h milling period. Later experiments were all conducted using this procedure.

In runs without the water seal, the powder was recovered by simply opening the vial in a protective atmosphere to prevent condensation from ambient humidity. For experiments with the water seal, the vials were first placed in a vacuum chamber to sublimate the ice.

Product powders were characterized using various techniques. X-ray diffraction (XRD) measurements were conducted on a Philips X'pert MRD powder diffractometer using unfiltered Cu radiation (λ=1.5438 Å), operating at 45 kV and 40 mA. XRD provided information about the phase composition of the prepared materials; in particular, identification of any products of partial thermite reaction occurring during the milling was of interest. Particle size distributions (PSD) were measured by light scattering using a Beckman-Coulter LS230 Particle Counter.

To study morphology of the prepared materials, powders were embedded in epoxy and cross-sectioned. After polishing, cross-sectioned samples were examined on a LEO 1530 Field Emission Scanning Electron Microscope (SEM) operated at 10 kV. For the 12Al·3CuO material, at least five representative SEM images of each sample were taken at a fixed magnification and processed to determine the average size distribution of CuO inclusions in the aluminum matrix.

Reactivity of the prepared materials was analyzed using differential scanning calorimetry (DSC) and a custom wire-ignition set up. DSC experiments were performed using a Netzsch Simultaneous Thermal Analyzer STA409PC. Samples were heated using different heating rates ranging from 2 to 20 K/min in argon environment. The custom wire-ignition apparatus is shown in Figure 1. Its operation was presented in detail elsewhere[17] and it is only briefly described below. A slurry is prepared with the powder being tested placed in hexane or another quickly evaporating hydrocarbon liquid. A thin layer of the slurry is coated on a portion of a Nichrome® wire with a paintbrush and dried. The wire is then heated electrically with heating rates varying from 100 to 50,000 K/s. The wire temperature is monitored in real time using an infrared pyrometer. Simultaneously, the emission from the powder coating is measured with a photodiode, and the instant of powder ignition is detected by a spike in the photodiode signal. Thus, ignition temperatures at different heating rates are measured.

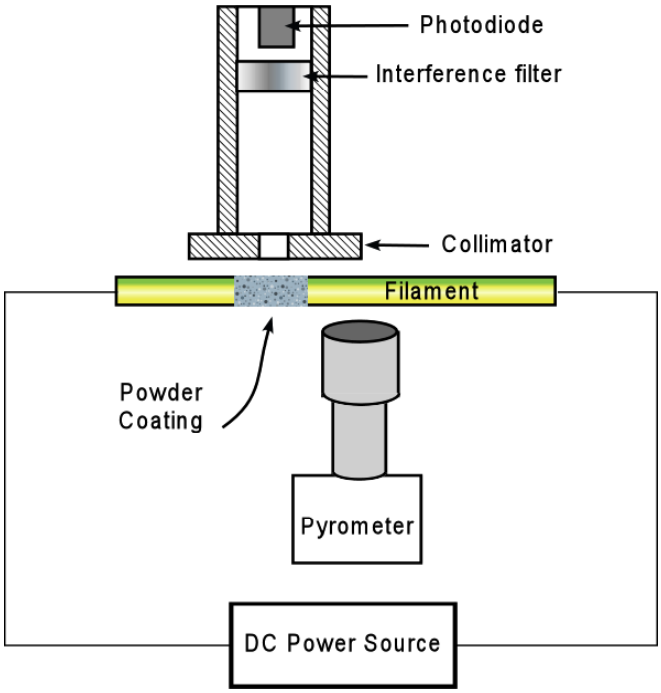

Figure 1. Simplified diagram of the heated filament ignition set up.

III. Preliminary Experiments and Results

Early cryogenic milling experiments used a nanocomposite powder with composition 12Al·MoO_3 prepared using a planetary mill as a starting material. The goal of these experiments was to establish whether measurable changes in the material morphology and particle size can be detected. Four milling vials 7/8" diameter, 3 7/8" length, were used in each milling run. The four milling vials are stacked in an array with two on the bottom and two on the top. It was observed that the powder milling occurs differently, depending on the location of the milling vial. Specifically, the powders were refined faster in the vials placed on the top of the vial array.

Considering powders prepared in the top vials, the change in morphology of the nanocomposite powder was undetectable. However, the particle sizes were found to change as a function of the milling time. Based on these observations, a milling progress function was considered to compare experiments with varied milling conditions. Similarly to the specific milling dose considered elsewhere[18], it was assumed that the milling progress function □ is proportional to the milling time *t*, the operating frequency of the mill *f*, as a measure of the energy of individual collisions, the number of milling media units present, *n*, proportional to the number of collisions, and the inverse of the powder mass *m*:

$$\Phi = n \cdot f \cdot t / m$$

Figure 2 shows the moments of the measured particle size distributions as a function of the progress function for a series of runs with nanocomposite 12Al·MoO_3 used as a starting material. As mentioned above, for these initial experiments consistent differences in the milling progress were observed between the vials placed in different positions within the mill. In Fig. 2 each run is represented by the 10th and the 90th percentiles of the volume-based size distribution, and by the median. Horizontal lines show respective values for the initial powder. It can be seen that maximum and median particle sizes systematically decrease as a function of the milling progresses.

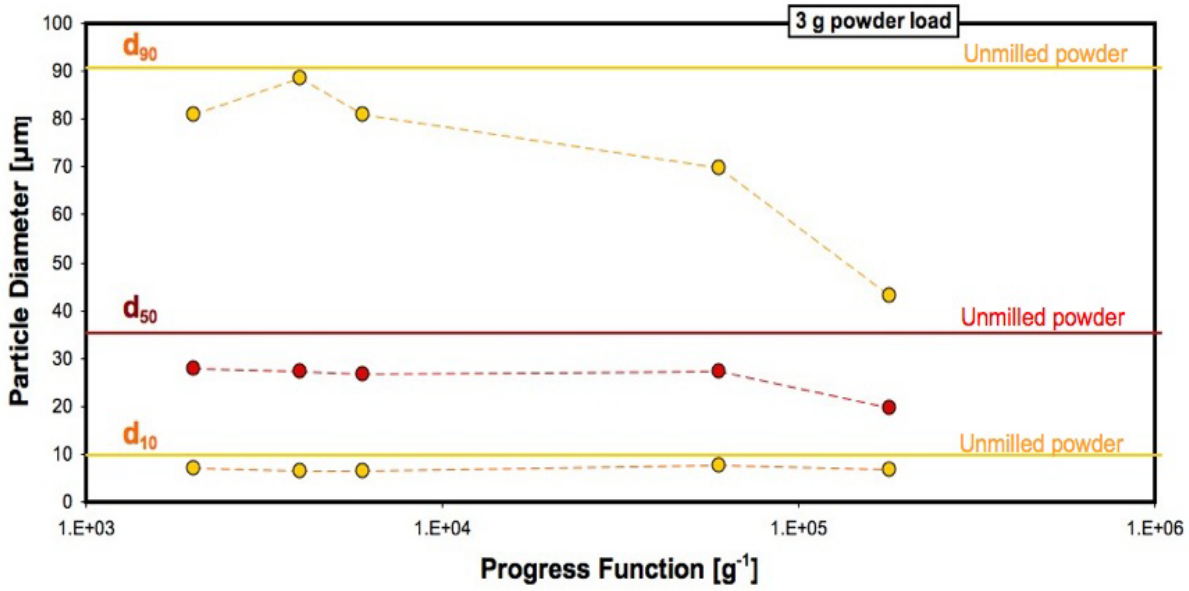

Figure 2. Progress function for preliminary experiments with 12Al·MoO_3 composite processed in top vials. At increasing progress function values, the particle diameter decreases. The percentiles for the composite powder used as starting material are shown for comparison.

No clear improvement in the rate of powder refinement was observed for using milling balls as compared to the cylindrical impactor. Note that the experimental results were most significantly affected by the location of the milling vial (top vs bottom position), while this position was not considered as a meaningful experimental parameter and thus was not recorded in the initial tests. The difference between the milling in top and the bottom vials is best illustrated in a follow-up set of experiments. The morphologies of powders produced as a result of direct milling of starting Al and CuO powders are shown in Fig. 3. The cross-sections shown in Fig. 3 are for powders prepared under identical conditions, but retrieved from different vials of the same milling run. The sample shown on the left side of Fig. 3 appears to

be only at the initial stage of the material refinement. Deformed from its initial shape, flake-like particles of Al are mixed with unattached (brighter) CuO inclusions with only few particles forming composite structure. The sample shown on the right side, however, is seen to contain a uniform nanocomposite material. Systematic investigation of this problem revealed that the temperature variation between the vials was the main factor affecting milling efficiency, although the presence of liquid nitrogen inside the vials due to non-hermetic sealing may also have played a role. The difference in temperature was associated with slow but continuous loss of liquid nitrogen from the milling compartment due to its evaporation. Thus, the top two vials were immersed into the liquid nitrogen only for a portion of the entire milling time and the effective temperature in the top two vials was somewhat higher than that in the bottom two vials, which remained in liquid nitrogen for the entire milling time. The temperature difference was expected to be small because all vials were placed in a thermally insulated compartment of the freezer mill containing liquid nitrogen. In further experiments, the level of liquid nitrogen was maintained constant during the entire milling period. The experiments were stopped periodically, the milling compartment was opened and the liquid nitrogen refilled.

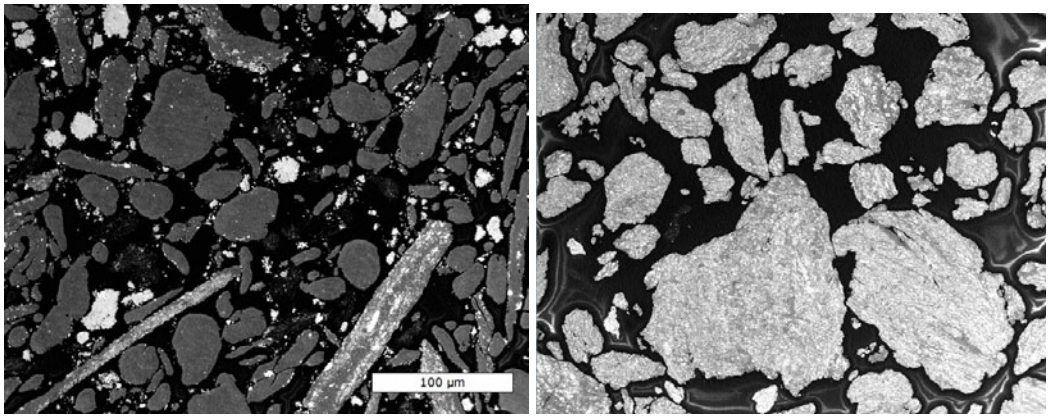

Figure 3. Backscattered electron images of two 12Al·3CuO milled under nominally identical conditions. The images have the same magnification. The sample on the left was retrieved from a lower vial, while the one on the right was retrieved from an upper vial. The powders were milled using a combination of 3 7/16" and 10 3/16" steel balls.

It was further found that when the temperature was maintained constant, manufacturer-provided cylindrical steel impactor operated in a similar fashion for the vials placed in both top and bottom positions. However, the powder refinement with steel balls used as milling tools depended on the vial position even if the liquid nitrogen level was maintained constant during the experiment.

Note that most of the experiments described below were performed before the effects of the milling tools and position of the vials were well understood. As the number of experiments increased it became clear that the milling in the vials placed on top of the vial array results in a more consistent powder processing using both cylindrical impactor and milling balls. Thus, the results described below are for the experiments performed in the top vials only.

IV. Results and Discussion

The results are discussed in the context of comparing the properties of two nanocomposite materials with the same bulk composition of 12Al·3CuO. One of the materials was prepared using milling at cryogenic temperatures and the other was prepared using a planetary mill operated at room temperature. The same starting powders of Al and CuO were used to prepare both materials.

Material Characterization

The size distributions for starting powder blend used in both cryogenic and planetary mills, and for both produced composite powders are shown in Fig. 4. The particle size distribution for the powder prepared in the planetary mill is somewhat narrower than the initial size distribution of the powder blend. Alternatively, the composite powder prepared at the cryogenic temperature appears to include quite a few relatively coarse particles. Note that the volume fractions of the particle size distributions shown in Fig. 4 are heavily affected by larger particles.

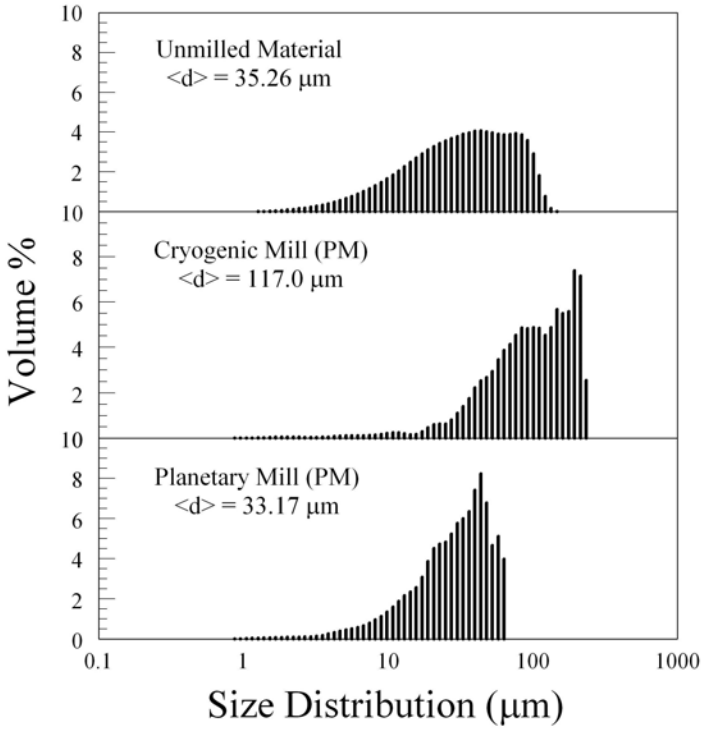

Figure 4. Particle Size Distribution of unmilled 12Al·3CuO in comparison to cryomilled and planetary milled materials. The figure indicates that particle sizes for cryomilled materials were not as fine as the planetary or starting material.

To compare the morphology of two prepared materials, the size distributions of CuO inclusions in Al matrix were measured using processing of the SEM images of the particle cross-sections. Representative SEM images are shown in Fig. 5. Images for the powders produced in both planetary and cryogenic mills showed brighter CuO inclusions within the darker Al matrix. The major apparent difference between the images is that the cryomilled material seems to be more homogeneous in terms of the distribution of CuO inclusions as compared to the material prepared in the planetary mill. The sizes of the CuO inclusions do not appear to be substantially different. This is confirmed by the size distributions shown in Fig. 6. These distributions were obtained by image processing.. The images were thresholded, lighter objects (CuO inclusions) were

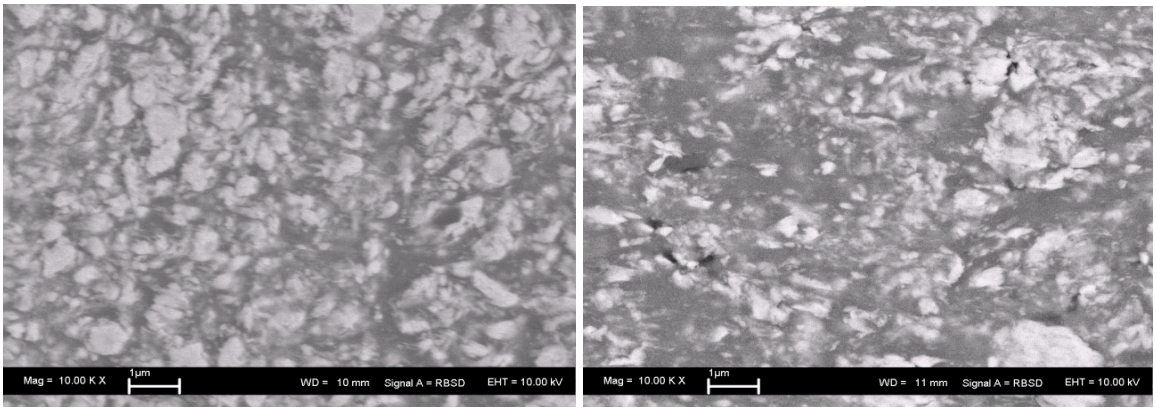

Figure 5. Backscattered electron images of 12Al·3CuO nanocomposites. The material on the left was cryomilled, and the material on the right was milled at room temperature in a conventional planetary mill. In both images, bright inclusions are CuO, while the dark matrix is Al.

selected, and their Feret diameters was automatically determined using the UTHSCSA ImageTool package by S. Brent Dove available as freeware In both cases, the inclusions size distributions peak at around 160 nm. The magnification used to collect the SEM images restricted the capability to resolve finer inclusions, so that the measurements are likely biased to the larger inclusion sizes. This limitation is manifested by an apparent sharp drop off in the count number for inclusions under 80 nm. Thus, the difference in the mean inclusion size identified for the two powders is considered to be insignificant, and the inclusion size distributions are seen as effectively equivalent for both powders.

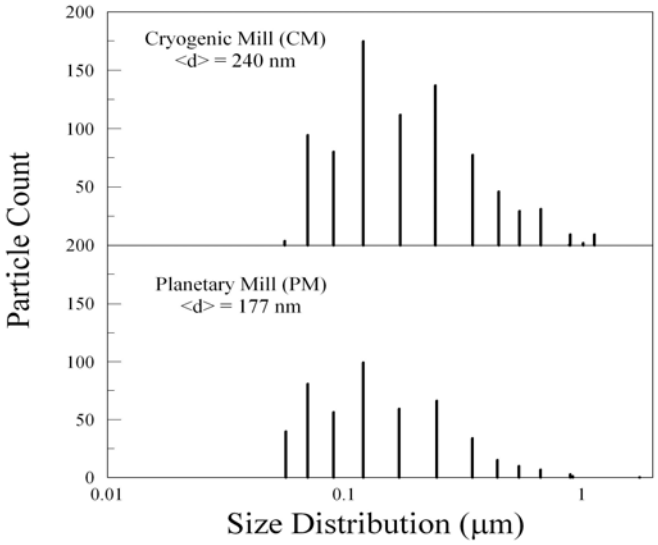

Figure 6. Inclusion Size Distribution for 12Al3CuO cryomilled and planetary milled. Both materials have similar distributions and evidence of analysis limitations by the sharp drop left of the peak.

Figure 7 shows XRD patterns collected for the powders prepared in the cryogenic and planetary mills. The differences between the patterns are subtle. The strongest peaks are, not unexpectedly, produced by the CuO and Al structures for both materials. However, the measured peak intensities are lower for the material prepared in the cryogenic mill. In addition, the peaks are wider for the material prepared at cryogenic temperatures, both indicators pointing out at a finer crystallite size for these materials as compared to their counterparts prepared in the planetary mill. A weak increase in the baseline indicating the presence of minor amounts of poorly crystalline aluminum oxides was occasionally observed for the powders prepared in the planetary mill. Such oxides could have formed as a result of undesirable thermite reaction occurring locally in the vial during the milling. Similar features were never detected for the powders prepared in the cryogenic mill.

Material Reactivity

DSC traces are shown in Figure 8. Traces for both powders were measured at different heating rates in argon. It is observed that for both materials a relatively weak endothermic feature precedes the observed exothermic peak. However, the DSC traces are substantially different for the powders prepared at different milling temperatures. The endothermic peak is substantially stronger for the powder prepared at the cryogenic temperature. This peak occurs around 820 K and its position does not shift to higher temperatures at higher heating rates. Based on its parameters, this peak is assigned to a eutectic point between Al and the $CuAl_2$ alloy in the binary Al-Cu system[19]. In order for this transition to occur, the $CuAl_2$ alloy must have formed prior, indicating that some of the copper was reduced and available to react with aluminum. Thus, the presence of a stronger endothermic feature corresponding to the eutectic reaction for the material prepared at the cryogenic temperature indicates its higher reactivity at lower temperatures, compared to the material prepared in the planetary mill. Indeed a raised baseline observed clearly for the cryomilled material prior to the endothermic peak supports this reaction sequence.

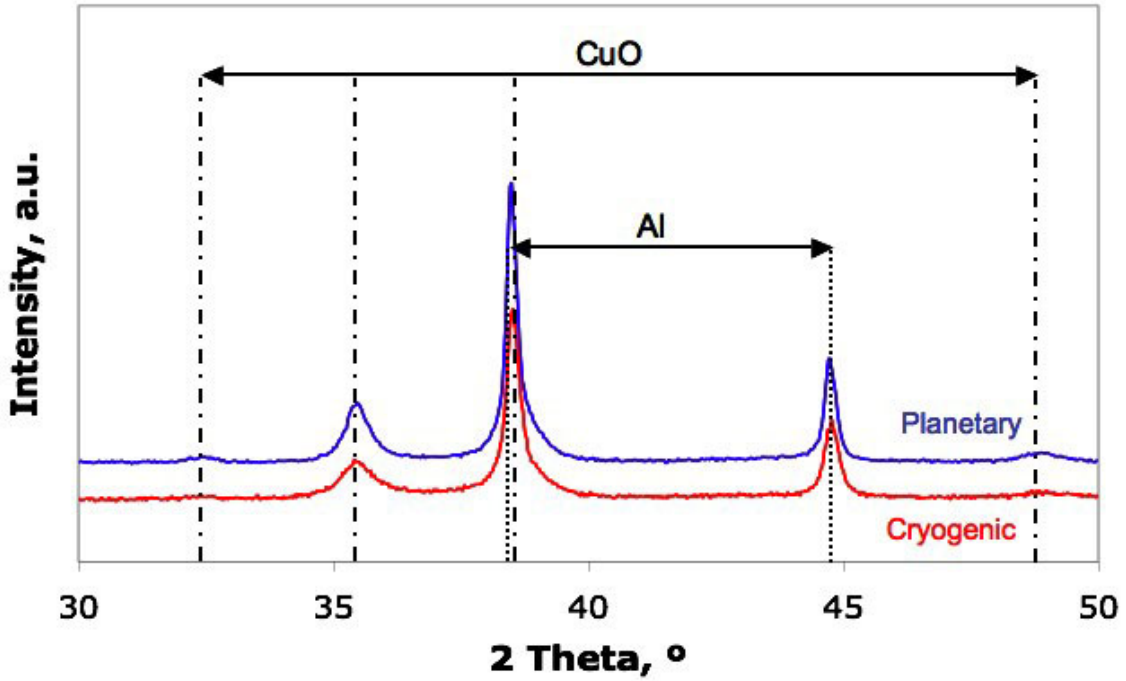

Figure 7. XRD traces for both cryogenic and planetary mill. Both materials are very similar in composition with differences in the peak widths and intensity. This suggests that milling cryogenically will result in more refined components.

The second important difference in the DSC signals for the two materials has to do with the main exothermic peak clearly visible in all DCS traces. For the cryomilled material, this peak occurs at significantly lower temperatures as compared to that for the material prepared in the planetary mill. Furthermore, the kinetic shift to higher temperatures at increased heating rates is smaller for the material prepared at cryogenic temperatures, indicating that the equivalent activation energy for the exothermic reaction is higher as compared to the material prepared in the planetary mill.

The results of the heated filament ignition experiments are shown in Fig. 9. Both materials were heated at different heating rates. In both cases, the measured ignition temperatures are

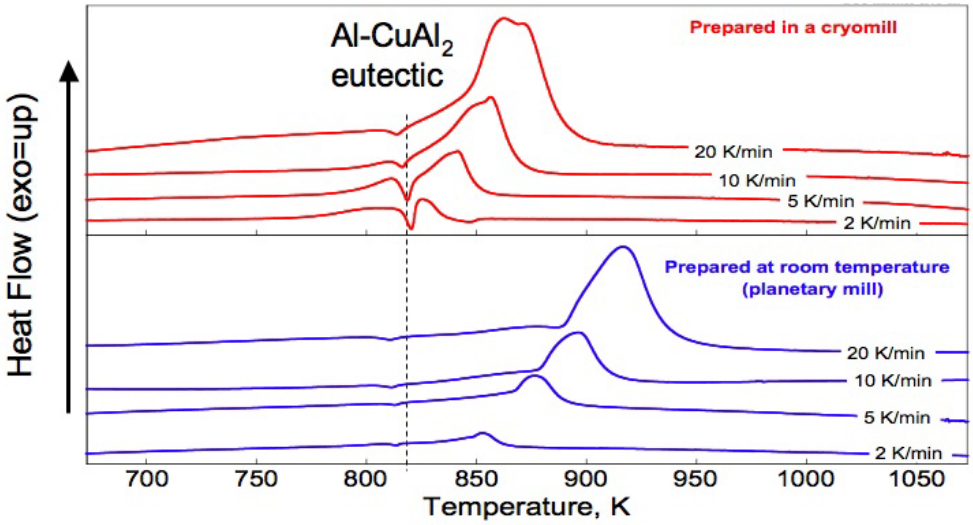

Figure 8. Differential scanning calorimetry traces measured at various heating rates for materials prepared in cryogenic mill and planetary mill.

close to the temperature range in which the eutectic melting of Al and $CuAl_2$ alloy occurs in the binary Al-Cu system. However, the observed effect of the heating rate on the ignition temperature is greater for the material prepared at cryogenic temperature. It can be initially proposed that the ignition in the material prepared in the planetary mill is controlled by the eutectic melting in the sample, while for the material prepared in the cryomill the reaction may be thermally activated and may initiate even before the eutectic melting.

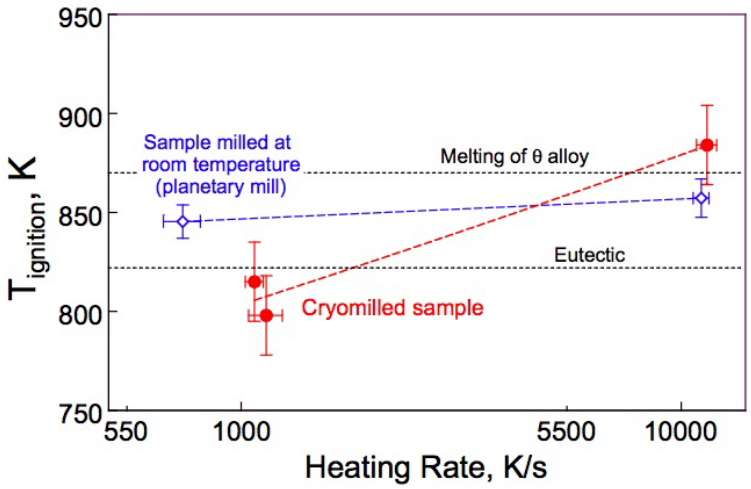

Figure 9. Ignition temperatures measured as a function of the heating rate in the heated filament ignition experiments.

IV. Conclusions

The feasibility of preparing reactive nanocomposite materials by ARM performed at cryogenic temperatures is established. The inclusions of the harder phase (metal oxide) distributed in the matrix of a softer component (aluminum) are approximately of the same size for materials prepared at both cryogenic and room temperatures. However, the inclusions are distributed more uniformly for the materials prepared in the cryomill. X-ray diffraction analysis shows that the crystallite sizes of the components mixed by ARM performed at the cryogenic temperature are finer compared to their counterparts produced by the room temperature milling. It is also observed that effectively no reacted material can be detected in the nanocomposite prepared at the cryogenic temperature. Thermal analysis indicated that the material prepared at cryogenic temperatures is more reactive at low temperatures. It is also observed that the reaction mechanisms and activation energies differ for the materials with the same bulk chemical composition prepared at different temperatures.

V. Acknowledgement

This work was supported in parts by Defense Threat Reduction Agency and by RDECOM-ARDEC, Picatinny.

VI. References

1. Puszynski JA, Bulian CJ, Swiatkiewicz JJ. The Effect of Nanopowder Attributes on Reaction Mechanism and Ignition Sensitivity of Nanothermites. Materials Research Society Symposium Proceedings 2006; 896:147-58.
2. Tillotson TM, Gash AE, Simpson RL, Hrubesh LW, Satcher Jr. JH, Poco JF. Nanostructured energetic materials using sol-gel methodologies. Journal of Non-Crystalline Solids 2001; 285(1-3):338-45.
3. Danen WC, Jorgensen BS, Busse JR, Ferris MJ, Smith BL. Los Alamos nanoenergetic metastable intermolecular composite (super thermite) program. 221st ACS National Meeting, San Diego, CA, United States, Abstracts of Papers, 2001.
4. Perry WL, Tappan BC, Reardon BL, Sanders VE, Son SF. Energy release characteristics of the nanoscale aluminum-tungsten oxide hydrate metastable intermolecular composite. Journal of Applied Physics 2007; 101(6):064313/1-064313/5.

5. Prakash A, McCormick AV, Zachariah MR. Synthesis and reactivity of a super-reactive metastable intermolecular composite formulation of Al/$KMnO_4$. Advanced Materials 2005; 17(7):900-3.
6. Walter KC, Pesiri DR, Wilson DE. Manufacturing and performance of nanometric Al/MoO_3 energetic materials. Journal of Propulsion and Power 2007; 23(4): 645-50.
7. Pantoya ML, Granier JJ. Combustion behavior of highly energetic thermites: Nano versus micron composites. Propellants, Explosives, Pyrotechnics 2005; 30 (1):53-62.
8. Dreizin EL, Schoenitz M. Nano-composite energetic powders prepared by arrested reactive milling. US Patent Application 20060053970; published in March 2006.
9. Schoenitz M, Ward TS, Dreizin EL. Fully Dense Nano-Composite Energetic Powders Prepared By Arrested Reactive Milling. Proceedings of The Combustion Institute 2005; 30:2071-8.
10. Umbrajkar S, Trunov MA, Schoenitz M, Dreizin EL, Broad R. Arrested Reactive Milling Synthesis and Characterization of Sodium-Nitrate Based Reactive Composites. Propellants, Explosives, Pyrotechnics 2007; 32(1):32-41.
11. Dreizin EL, Schoenitz M, Shoshin YL, Trunov MA. Highly-Energetic Nanocomposite Powders Produced by Arrested Reactive Milling. Internaional Annual Conference of ICT 2005, 36^{th} (Energetic Materials), p. 138/1-138/12.
12. Umbrajkar SM, Schoenitz M, Dreizin EL. Control of Structural Refinement and Composition in Al-MoO_3 Nanocomposites Prepared by Arrested Reactive Milling. Propellants Explosives and Pyrotechnics 2006: 31(5):382-9.
13. Umbrajkar SM, Seshadri S, Schoenitz M, Hoffmann VK, Dreizin EL. Aluminum-Rich Al-MoO_3 Nanocomposite Powders Prepared by Arrested Reactive Milling. Journal of Propulsion and Power 2008; 24(2)192-8.
14. Umbrajkar SM, Schoenitz M, Jones SR, and Dreizin EL, Effect of Temperature on Synthesis and Properties of Aluminum-Magnesium Mechanical Alloys. Journal of Alloys and Compounds 2005; 40(1-2)70-77
15. Perez, RJ, Huang B, Lavernia EJ. Thermal Stability of Nanocrystalline Fe-10 wt.% Al Produced by Cryogenic Mechanical Alloying. Nanostructured Materials 1996; 7 (5) 565-572
16. Witkin, DB, Lavernia EJ. Synthesis and mechanical behavior of nanostructured materials via cryomilling. Progress in Materials Science 2006; 51 (1)1-60
17. Ward, TS, Trunov, MA, Schoenitz, M, Dreizin, EL, Experimental methodology and heat transfer model for identification of ignition kinetics of powdered fuels. International Journal of Heat and Mass Transfer 2006; 49(25-26) 4943-4954
18. Ward, TS, Chen, W, Schoenitz, M, Dave, RN, Dreizin, EL. A study of mechanical alloying processes using reactive milling and discrete element modeling. Acta Materialia 2005; 53(10), 2909-2918.
19. Massalski, TB., The Al−Cu system. Journal of Phase Equilibria, 1980 1(1) 27-33